



Published in final edited form as:

Mol Psychiatry. 2017 December ; 22(12): 1714–1724. doi:10.1038/mp.2016.155.

PDE11A negatively regulates lithium responsivity

G. Pathak¹, M.J. Agostino², K. Bishara¹, W.R. Capell¹, J.L. Fisher¹, S. Hegde¹, B.A. Ibrahim¹, Kaitlyn Pilarzyk¹, C. Sabin¹, Taras Tuczkewycz^{3,‡}, Steven Wilson¹, and M.P. Kelly^{1,*}

¹ University of South Carolina School of Medicine, Columbia, SC 29016

² Pfizer, Andover, MA 01810

³ Pfizer, Groton, CT 00640

Abstract

Lithium responsivity in patients with bipolar disorder has been genetically associated with *Phosphodiesterase 11A (PDE11A)*, and lithium decreases *PDE11A* mRNA in iPSC-derived hippocampal neurons originating from lithium responsive patients. PDE11 is an enzyme uniquely enriched in the hippocampus that breaks down cAMP and cGMP. Here, we determined if decreasing PDE11A expression is sufficient to increase lithium responsivity in mice. In dorsal hippocampus (DHIPP) and ventral hippocampus (VHIPP), lithium-responsive C57BL/6J and 129S6/SvEvTac mice show decreased PDE11A4 protein expression relative to lithium-unresponsive BALB/cJ mice. In VHIPP, C57BL/6J mice also show differences in PDE11A4 compartmentalization relative to BALB/cJ mice. In contrast, neither PDE2A nor PDE10A expression differ among the strains. The compartment-specific differences in PDE11A4 protein expression are explained by a coding SNP at amino acid 499, which falls within the GAF-B homodimerization domain. Relative to the BALB/cJ 499T, the C57BL/6J 499A decreases PDE11A4 homodimerization, which removes PDE11A4 from the membrane. Consistent with the observation that lower PDE11A4 expression correlates with better lithium responsiveness, we found that *Pde11a* KO mice given 0.4% lithium chow for 3+ weeks exhibit greater lithium responsivity relative to WT littermates in tail suspension, an antidepressant predictive assay, and amphetamine hyperlocomotion, an anti-manic predictive assay. Reduced PDE11A4 expression may represent a lithium-sensitive pathophysiology, because both C57BL/6J and *Pde11a* KO mice show increased expression of the pro-inflammatory cytokine IL-6 relative to BALB/cJ and PDE11A WT mice, respectively. Our finding that PDE11A4 negatively regulates lithium responsivity in mice suggests that the *PDE11A* SNPs identified in patients may be functionally relevant.

Users may view, print, copy, and download text and data-mine the content in such documents, for the purposes of academic research, subject always to the full Conditions of use:http://www.nature.com/authors/editorial_policies/license.html#terms

*corresponding author Michy P. Kelly, Ph.D., Department of Pharmacology, Physiology & Neuroscience, University of South Carolina School of Medicine, 6439 Garners Ferry Road, VA Bldg 1, 3rd Floor, D-12, Columbia, SC 29209, Phone: 803-216-3546, Fax: 803-216-3551.

‡Current affiliation: Taras Tuczkewycz, Research Support, ITox, Charles River Laboratories, 50 Northern Ave, Boston, MA 02210, Building 1 5001-O, T: (617) 961-8407, C: (860) 331-1593, Taras.Tuczkewycz@vrtx.com

MPK received consulting fees from ASUBIO, Inc. and Deallus for projects unrelated to the current manuscript and is a former employee of Pfizer. MJA is an employee of Pfizer. TT is a former employee of Pfizer and is currently an employee of Charles River. Remaining authors have no financial conflicts to disclose.

Keywords

PDE11; PDE2; PDE10; fractionation; bipolar disorder; lithium; hippocampus; phosphodiesterase

INTRODUCTION

Lithium is argued to be the best treatment option for patients with bipolar disorder, but it has a narrow therapeutic window due to significant side effect liability [1]. If we could selectively augment the beneficial mood stabilizing effects of lithium in the brain without increasing its harmful peripheral side effects, we might be able to improve the safety margin of lithium treatment for patients with bipolar disorder because mood stabilization could be achieved with systemically lower doses. One way to achieve this selective augmentation of lithium's positive effects is to target a molecule that is selectively expressed in the brain.

Phosphodiesterase 11A (PDE11A) hydrolyzes cAMP and cGMP equally well [2, 3] and is the only PDE to be preferentially expressed in the hippocampus [4-6]. We have shown in rodents that PDE11A4, the longest PDE11A isoform, is almost exclusively expressed in CA1 and subiculum of the ventral hippocampus (VHIPP), with minimal expression in the dorsal HIPP (DHIPP) [4, 6] and little to no protein expression outside of the brain [5]. Genetic findings in humans suggest a role for *PDE11A* in brain function [7-12] (but see [13, 14]). For example, *PDE11A* single nucleotide polymorphisms (SNPs) have been associated with major depression and antidepressant response [7-9] (but see [13, 14]). Of particular interest to the present study, PDE11A SNPs have been associated with lithium responsiveness in patients with bipolar disorder [10, 11], a *PDE11A* inactivating mutation has been associated with increased suicide risk [12]—a symptom lithium uniquely reduces in patients with bipolar disorder [15], and lithium decreases *PDE11A* mRNA expression in iPSC-derived hippocampal neurons originating from lithium-responsive patients but not from lithium-unresponsive patients [16].

A relationship between lithium and cyclic nucleotide signaling is well precedented. Lithium is known to modulate cyclic nucleotide signaling (c.f., [17]), and disturbances in cyclic nucleotide signaling have repeatedly been observed in patients with bipolar disorder (e.g., [18-26]). Interestingly, the alterations in cyclic nucleotide signaling identified in patients with bipolar disorder can be subcellular-compartment specific [18, 23, 25], as can be the effects of lithium on cyclic nucleotide signaling [27-29]. Therefore, we determined if PDE11A expression and/or compartmentalization differ between mouse strains that respond well versus poorly to lithium. Further, we determined if differences in PDE11A compartmentalization are due to a nonsynonymous coding SNP that exists between mouse strains at amino acid 499, which is positioned within the GAF-B homodimerization domain. We also established if decreasing PDE11A expression is sufficient to strengthen the antidepressant-like effects of lithium in the tail suspension test (TST) and the anti-manic-like effects of lithium in amphetamine-stimulated hyperactivity by testing *Pde11a* wild-type (WT) and knockout (KO) mice. Finally, we determined if PDE11A controls protein expression of the proinflammatory cytokine IL-6, a potential mood disorder biomarker

[30-37], to clarify whether PDE11A holds promise as a possible target for adjuvant treatment or simply as a patient selection marker.

METHODS

Subjects

C57BL/6J (The Jackson Laboratories (JAX); Bar Harbor, ME), BALB/cJ (JAX) and 129S6/SvEvTac mice (Taconic; Hudson, NY) were ordered in at 10-12 weeks or bred onsite. All C57BL/6J, BALB/cJ and 129S6/SvEvTac mice were group housed and habituated to the colony at least 1 week prior to sacrifice. mRNA analyses and protein analyses of the whole hippocampus using these strains were conducted on cohorts of all males; however, protein analyses on dorsal vs. ventral hippocampus were conducted on mixed cohorts of males and females (cohort used in Figure 1D-G and S3 = 50% female; cohort used in Figure 2, Figure 5A-C, and S2C-F = 25% female). *Pde11a* KO mice were originally developed by Deltagen (San Mateo, CA), and are maintained on a mixed C57BL/6J-C57BL/6N-129S6/SvEvTac background, as previously described [6]. *Pde11a* mice used in behavioral experiments were bred at JAX in heterozygous (HT) × HT matings, with same-sex WT, HT, and KO littermates weaned together and shipped onsite at 8-12 weeks old. No more than 2 sets of sex-matched littermates (i.e., a WT, HT, KO trio) came from the same litter. Upon delivery, Cohort1 was single housed for consistency with previous reports [6] and was tested in TST and then amphetamine-stimulated locomotor activity. Cohort2 remained group housed and was tested only in TST. *Pde11a* mice used in biochemical studies were bred onsite at USC in HT × HT matings and were weaned and group housed as described above. In all KO studies, approximately equal numbers of males and females were used. Animals were housed on a 12:12 light:dark cycle and allowed *ad lib* access to food and water. See Figure Legends for n's. Sample sizes were selected based on previous experiences with these assays. Experiments were carried out in accordance with the National Institutes of Health Guide for the Care and Use of Laboratory Animals (Pub 85-23, revised 1996) and were fully approved by the Institutional Animal Care and Use Committees of the University of South Carolina and Pfizer.

Protein sample preparation

Animals were sacrificed by cervical dislocation and brain regions immediately dissected onto dry ice and stored at -80°C . As previously described [4], tissue samples and cell lysates were homogenized in ice-cold lysis buffer (20 mM Tris-HCl, pH 7.5; 2 mM MgCl_2 ; Thermo Pierce Scientific phosphatase/protease inhibitor tablet) using a probe sonicator. For immunoprecipitation (IP), lysis buffer also contained 0.5% Triton X-100/150 mM NaCl, with IP performed using Protein A and Dynabeads as per manufacturer's instructions (Life Technologies; Bedford, MA). For Native polyacrylamide gel electrophoresis (PAGE), lysates were additionally nutated for 30 minutes at 4°C with 0.5% Triton X-100, treated with 0.1ul/ml (v/v) Thermo Pierce nuclease for 15 minutes at room temperature, and centrifuged at $20,000g$ for 30 minutes at 4°C . For fractionation, homogenates were spun at $1,000g \times 10$ minutes at 4°C to remove nuclear fractions. Supernatants were then centrifuged at $89,000 \text{ rcf} \times 10$ minutes at 4°C to yield a cytosolic supernatant fraction. The pellet was washed with a 2nd resuspension, centrifuging, and subsequent rinse with ice-cold lysis buffer. The pellet

was then sonicated in ice-cold lysis buffer + 0.5% Triton X-100, nutated for 30 minutes at 4°C, and centrifuged at 60,000 rcf × 30 minutes at 4°C to yield the soluble membrane supernatant fraction. Samples were stored at –80°C until use. Protein levels were quantified using the DC Protein Assay kit (BioRad, Inc.; Hercules, CA) as per manufacturer’s instructions.

Western blotting

Lysates were run on either denaturing NuPAGE Novex 4-12% Bis-Tris or NativePAGE Novex 4-16% Bis-Tris gels, as per manufacturer’s instruction (Life Technologies). Blots were probed overnight at 4°C with antibodies recognizing PDE11A (1:500, PD11A-112AP FabGennix—Frisco, TX [4-6]), PDE2A (1:1000, PD2A-101AP FabGennix [38]), PDE10A (1:2500, Enzo Life Science; Farmingdale, NY [39]), actin (1:10,000, A2066 Sigma; St. Louis, MO), IL-6 (1:200, MAB406 R&D Systems; Minneapolis, MN [40]), GFP (1:2000, sc-8334 Santa Cruz; Dallas, TX), or RFP (1:10,000, A00682 Genscript). Blots were then processed as previously published [4, 6, 41].

In situ hybridization

Animals were sacrificed by cervical dislocation. Brains were cryosectioned at 20 µm and autoradiography for the various PDEs was performed as previously reported [4-6, 38, 42]. For *Ahrgap32* autoradiography was similarly performed using the following antisense probe (3'-AGCCCTGTTTGAGTCAGTCTCAGTGAGAGCTCTCTG-5', NM_177379.4), the specificity of which was confirmed by obtaining identical labeling with a second antisense probe sequence and no signal with the sense version of the probes.

Plasmid generation

Plasmids encoding either mouse *Pde11a4* (NM_001081033; 499A) with N-terminally fused *EmGFP*[43] (A206Y mutation introduced to prevent EmGFP dimerization) or an isolated *Pde11a4* GAF-B domain (aa388-558 of NP_001074502.1, which includes 14 upstream amino acids as a spacer) with N-terminally fused *mCherry* [44] were synthesized in pUC57 by Genscript (Township, NJ) and subsequently subcloned into pcDNA3.1+ mammalian expression vectors (Life technologies). 499T/499D mutations were generated using the QuikChange procedure and products (Agilent Technologies, Santa Clara, CA). Oligonucleotide primers were synthesized by Integrated DNA Technologies (Coralville, IA) and mutations were verified by DNA sequencing (Functional Biosciences, Madison WI). Similar constructs expressing only *EGFP* or *mCherry* were used as controls.

Cell culture and transfections

COS-1 and HEK293T cells (ATCC; Manassas, VA) were grown in 24-well plates or 100mm dishes containing Glutamax media (GIBCO; Gaithersburg, MD)/10% fetal bovine serum (FBS) at 37°C/5% CO₂. Plasmid DNA was transiently transfected using Optimem and Lipofectamine 2000 as per manufacturer’s instructions (Life Technologies). The morning following transfection, Optimem was replaced with Glutamax media/5% FBS and cells continued to grow for 5-24 hours. Cells were fixed with 4% paraformaldehyde for imaging

studies or harvested in lysis buffer for Westerns. Experiments shown in Figures 3D-O were repeated 3 times with similar results.

Microscopy

For data collection, cells were imaged using a Leica HC PL Fluotar 10X/0.3 ∞ /-D objective on an inverted Leica DMIL microscope. 1 digital picture per well or dish was collected using NIS-Elements BR-2.30, and an experimenter blind to treatment then categorized the EmGFP-PDE11A4 expression pattern for each labeled cell in the image (cytoplasmic-only vs. containing aggregates). Images shown in figure were collected using an LPI anFL PH2 40X/0.65 ∞ /1.2 objective on an EVOSfl digital microscope.

Drugs

Lithium carbonate and control diets were obtained from Harlan Teklad. [0.2%] and [0.4%] were selected based on previous work showing [0.4%] achieves clinically-relevant plasma exposures [45]. Mice were fed the chow for 3+ weeks and given access to 0.9% saline to mitigate potential ion imbalances [45]. A 1.78 mg/kg s.c. dose of D-amphetamine (Sigma Aldrich, salt corrected and dissolved in sterile saline at 10 mL/kg) was selected based on our previous experience [41, 46].

Behavior

To conduct tail suspension testing (TST), Scotch tape was wrapped around the mouse's tail and then affixed to the hook of a Hamilton-Kinder TS100 tail suspension system. The time spent immobile during a 6-minute trial was automatically recorded [47, 48]. Locomotor activity was recorded using the Accuscan Versamax system and Versadat software as previously described [6, 41, 46].

Data analyses

Data were collected in a blinded fashion, with technical variables counterbalanced across biological variables, and analyzed using Statistica 9.0 or Sigmaplot 11.1. As previously described [6, 41, 42], to mitigate non-specific effects related to transfer efficiencies, film exposures, etc. across gels, Western blot data on a given gel were normalized to a reference group (e.g., WT). Data were analyzed by analysis of variance (ANOVA), repeated measure ANOVA, Student t-test (t), Mann Whitney Rank Sum (T), Wilcoxon Signed Rank Test (Z), or Pearson Product Moment Correlation as appropriate. T-tests were 2 sided. NOTE: where parametric tests failed equal variance or normality, nonparametric tests were used. Data were analyzed for effect of strain, brain region, fraction, plasmid, genotype, and/or sex where n's were sufficient to examine a potential effect of sex (i.e., if $n > 8$ /sex/group). In cases of significant ANOVAs, *post hoc* analyses were conducted using the Student-Newman-Keuls Method. As previously described [6, 41, 42, 49], statistical outliers > 2 standard deviations from the mean were removed from analyses (Figure 2B, 1 of 16 subjects; Figure 3K, 1 of 72 samples; Figure 3N, 1 of 15 data points; Figure 3O, 2 of 22 data points; Figure 4A, 1 of 36 data points; Figure 4C, 1 of 77 subjects; Figure 5B, 2 out of 32 data points; Figure 5C, 1 out of 32 data points; Figure 5E, 2 of 36 subjects). Significance was defined as $P < 0.05$.

RESULTS

C57BL/6J mice, which respond well to lithium, express significantly lower levels of PDE11A4 than do BALB/cJ mice, which respond poorly to lithium

PDE11A4 expression and compartmentalization were measured in the hippocampi of mice that respond well (C57BL/6J), moderately (129S6), or poorly to chronic lithium (BALB/cJ) [45, 50]. *Pde11a4* mRNA expression is significantly lower in the C57BL/6J and 129S6/SvEvTac mice relative to the BALB/cJ mice, but only in dorsal (d) and not ventral (v) CA1 (Figure 1A; $F(2,17)=7.15$, $P=0.006$). These differences in *Pde11a4* mRNA expression were confirmed in a 2nd cohort of mice (Figure S1). Similarly, C57BL/6J and 129S6/SvEvTac mice express significantly less PDE11A4 protein relative to BALB/cJ mice in both DHIPP and VHIPP (Figure 1D-G; $F(2,33)=12.29$, $p<0.001$), despite the lack of difference in *Pde11a4* mRNA expression between the strains in VHIPP (Figure 1A, S1A-B). Further, all 3 strains mice demonstrate far more expression of PDE11A4 protein expression in VHIPP vs. DHIPP (Figure 1D-G; $F(1,33)=622.65$, $p<0.001$), despite the fact that BALB/cJ mice fail to show the prototypical 2-fold enrichment of *Pde11a4* mRNA in vCA1 vs. dCA1 [4-6] (Figure 1A, S1A-B). These differences in PDE11A4 protein expression were confirmed in a 2nd cohort of mice (Figure S2). In DHIPP, C57BL/6J mice show lower PDE11A4 protein expression relative to BALB/cJ mice in both the cytosolic and membrane compartments (Figure 2; $F(1,9)=11.13$, $p=0.005$). Interestingly, in VHIPP, C57BL/6J mice exhibit lower PDE11A4 protein expression relative to the BALB/cJ mice only in the membrane (Figure 2C; $F(1,14)=10.63$, $P=0.006$). These compartment-specific differences in PDE11A4 protein expression were confirmed in a 2nd cohort of mice (Figure S3). The substantial effect of mouse strain on PDE11A4 expression appears to be specific, because expression of PDE2A and PDE10A, the closest related PDEs with appreciable expression in the hippocampus, does not differ across these mouse strains (Figures 1 and S1-S2).

C57BL/6J mice compartmentalize PDE11A4 in VHIPP differently than do BALB/cJ mice due to a nonsynonymous coding SNP in the GAF-B homodimerization domain

To determine if genetic differences in the *Pde11a* sequence might drive the differential compartmentalization of PDE11A4 in VHIPP, we examined the mouse genome and SNPs using the UCSC Genome Browser [51] and the Jackson Laboratory Phenome Database (JLPD) [52]. First we determined if the C57BL/6J *Pde11a* gene demonstrated a SNP homologous to human rs7585543, which was linked to lithium responsiveness in patients with bipolar disorder [10, 11]. The text “rs7585543” was used as a query in the UCSC Genome Browser (genome.ucsc.edu) and the Multiz genomic alignments of 44 vertebrates were examined closely. Although sequences of many species align well in this region, 600 nucleotides of mouse sequence are absent. Next, SNPs between 29 mouse strains were identified in the JLPD using “Pde11a” as a text query. Only four SNPs differed between C57BL/6J and BALB/cJ (129S6/SvEvTac not included in database): three synonymous (rs27939960, rs27939959, rs27981607) and one non-synonymous (rs27963339). The rs27963339 polymorphism encodes an alanine at position 499 in C57BL/6J and a threonine in BALB/cJ. Human *PDE11A4* encodes an alanine at position 499, with only 1 variation (glycine; GCA→GGA) noted in 121,412 chromosomes sequenced (http://www.ncbi.nlm.nih.gov/SNP/snp_ref.cgi?locusId=50940, accessed 04/19/16, [53]).

Although non-coding SNPs can have functional consequences [54], the coding SNP was most likely to yield a differential compartmentalization signal because the SNP 1) leads to a non-phosphorylatable versus a phosphorylatable residue and 2) falls within the PDE11A4 GAF-B homodimerization domain [55]. Post-translational modifications and protein-protein binding are the 2 key mechanisms known to regulate PDE trafficking [39, 56, 57]. As such, we determined if 499A vs. 499T would differentially affect PDE11A4 homodimerization and if that, in turn, might lead to a differential compartmentalization of PDE11A4.

COS-1 cells were transiently transfected with plasmids containing *EmGFP-PDE11A4* encoding the C57BL/6J 499A, the BALB/cJ 499T, or a phosphomimic 499D (Figure 3A). Results were compared to those obtained when PDE11A4 homodimerization was disrupted by co-expressing a dominant-negative isolated GAF-B domain (Figure 3B-C). Disrupting homodimerization with the isolated GAF-B domain significantly decreases expression of full length PDE11A4 while generating an ~80 kDa proteolytic fragment (Figure S4). Thus, total PDE11A4 protein expression was equilibrated between the control mCherry and GAF-B treatments by adding twice the transfection reaction to the GAF-B treated cells (Figure S4A). Although 499T and 499D do not consistently differ from 499A in terms of total PDE11A4 protein expression (Figure S4A), they do consistently differ in the expression of specific PDE11A4 macromolecular complexes, as determined by Native PAGE. Relative to 499A, 499T and 499D increase expression of a ~242 kDa PDE11A4 complex (Figure 3D, F; $F(2,8) = 6.835$, $P=0.019$), a molecular weight consistent with an EmGFP-PDE11A4 homodimer. Indeed, disruption of homodimerization with the isolated GAF-B domain decreases expression of the ~242 kDa complex (Figure 3E, G; $t(10) = 4.041$, $P=0.002$).

Consistent with these effects on homodimerization, fluorescent microscopy reveals that 499T and 499D promote trafficking of PDE11A4 into aggregates in COS-1 cells ($F(2,21)=16.97$, $P<0.001$); whereas, the isolated GAF-B domain prevents aggregation (Figure 3 H-J; $t(10)=8.88$, $P<0.001$). 499T and 499D increase the percentage of cells that developed aggregates as opposed to increasing the total number of aggregates per cell or the average size of the aggregates. The ability of 499T and 499D to increase aggregation and the ability of the isolated GAF-B domain to decrease aggregation are also observed in HEK293T cells (499: $F(2,21)=38.95$, $P<0.001$; GAF-B: $t(6)=4.20$, $P=0.006$). Importantly, adding the isolated GAF-B domain to 499T and 499D completely blocks their ability to promote PDE11A4 aggregation in COS-1 cells (Figure 3H, K), further suggesting that 499T and 499D increase trafficking of PDE11A4 into aggregates by promoting homodimerization. Biochemical fractionations show that 499T and 499D shift PDE11A4 from the cytosol to the membrane relative to 499A (Figure 3L, N; ; $F(2,41) = 8.80$, $P<0.001$), directly mimicking PDE11A4 in VHIPP of C57BL/6J vs. BALB/cJ mice (Figure 2C). Further, disrupting homodimerization with the isolated GAF-B domain shifts PDE11A4 in the opposite direction—from the membrane to the cytosol (Figure 3M, O; $t(18) = 4.87$, $P<0.001$).

PDE11A KO mice exhibit alterations in cAMP signaling and are more sensitive to the antidepressant and anti-manic effects of lithium

As noted above, disturbances in cyclic nucleotide signaling have been repeatedly observed in patients with bipolar disorder (e.g., [18-26]). Direct measures of baseline cAMP signaling

in the hippocampus of lithium responsive versus nonresponsive patients is lacking; however, increased basal phosphorylation of cAMP response element binding protein (pCREB) expression has been noted in lymphoblasts of lithium responsive patients [24]. As such, we measured pCREB in PDE11A KO vs. WT littermates along with expression of an mRNA under the control of pCREB signaling (i.e., *Arhgap32*). We did not observe a significant difference in pCREB phosphorylation between PDE11A KO mice relative to WT littermates when examining the VHIPP as a whole (WT, 1.00 ± 0.07 A.U.; KO, 1.132 ± 0.08 A.U.; $n=18$ /genotype), likely due to the fact that PDE11A4 is only expressed within a subpopulation of neurons in CA1 and the subiculum [58]. We were, however, able to detect a significant decrease in *Arhgap32* mRNA when measuring expression in VCA1 specifically (Figure 4A; $t(15)=2.67$, $P=0.017$), a change that is consistent with a localized increase in pCREB phosphorylation [59, 60].

The ability of a drug to reduce immobility in TST is predictive of antidepressant-like activity [61], and the ability of a drug to decrease the hyperlocomotor effects of D-amphetamine is indicative of anti-manic or antipsychotic like effects [62, 63]. As we previously reported using single-housed mice [6], group-housed PDE11A KO mice showed no basal difference in TST immobility relative to WT mice when fed a control diet. Group-housed PDE11A KO mice do, however, exhibit decreased TST immobility in response to a 0.4% lithium chow while group-housed WT mice do not (Figure 4B; $F(2,49)=3.52$, $P=0.037$). Interestingly, when the colony is single-housed, all genotypes demonstrate a significant reduction in TST immobility in response to 0.4% lithium chow ($F(2,172)=9.41$, $P=0.003$), possibly because single housing decreases PDE11A4 expression in WT mice [58]. As previously reported [6], we found no effect of genotype on D-amphetamine stimulated hyperactivity when mice consumed a control chow diet (data not shown). When fed 0.4% lithium chow, however, PDE11A HT and KO mice demonstrate a significantly blunted hyperlocomotor response to D-amphetamine relative to WT littermates during the 70-minute ($F(2,70)=4.50$, $P=0.015$), 75-minute ($F(2,70)=6.76$, $P=0.002$), 80-minute ($F(2,70)=5.64$, $P=0.005$), 85-minute ($F(2,70)=5.12$, $P=0.008$) and 90-minute time bins ($F(2,70)=6.69$, $P=0.002$). Together, these data show that decreased PDE11A expression is sufficient to increase lithium responsiveness.

Lower PDE11A4 expression increases IL-6 expression

Lastly, we determined if PDE11A4 regulates expression of the proinflammatory cytokine IL-6, a potential mood disorder biomarker [30-37] whose elevated expression is reversed by lithium [35]. Relative to the lithium-unresponsive BALB/cJ mice, the lithium-responsive C57BL/6J mice express significantly higher levels of IL-6 in both cytosol ($t(14)=94$, $P=0.005$) and membrane of DHIPP ($t(13)=7.43$, $P<0.001$) but only in cytosol of VHIPP ($T(13)=76.00$, $P=0.001$; Figure 5A-C). In VHIPP of C57BL/6J and BALB/cJ mice, lower PDE11A4 expression in membrane correlates with higher IL-6 expression in cytosol (Figure 5D). In DHIPP, PDE11A KO mice demonstrate significantly higher IL-6 expression than do their paired sex-matched WT littermates (Figure 5E; $Z(32)=2.84$, $P=0.003$).

DISCUSSION

Here we show that PDE11A, an enzyme genetically associated with lithium responsivity in patients with bipolar disorder, negatively regulates lithium responsivity in mice. PDE11A4 expression in the DHIPP and VHIPP are significantly reduced in lithium-responsive C57BL/6J and 129S6/SvEvTac mice vs. lithium-unresponsive BALB/cJ mice (Figures 1-2, S1-S3), and behavioral experiments in *Pde11a* KO mice show decreasing PDE11A expression is sufficient to increase lithium responsivity (Figure 4). A key driver of the PDE11A4 expression differences noted between mouse strains is a nonsynonymous coding SNP falling within the PDE11A4 GAF-B domain, a mutation that alters rates of PDE11A4 homodimerization and compartmentalization (Figure 3). Our findings are consistent with a number of studies examining tissue from patients with bipolar disorder that describe significant changes in the cAMP cascade [18-26, 64, 65], including changes restricted to specific subcellular compartments [18, 23, 25] and changes associated with lithium responsivity [24, 66].

Strain differences in PDE11A4 compartmentalization are associated with genetically-driven differences in PDE11A4 homodimerization

We show that homodimerization is a key regulator of PDE11A4 subcellular compartmentalization (Figure 3). It has long been known that all PDEs homodimerize/oligomerize, but the functional significance of this interaction remained unknown [67]. Homodimerization of PDE11A4 does not alter its substrate affinity [55]; instead, it appears to control which pool of cyclic nucleotides PDE11A4 can degrade. We believe homodimerization/oligomerization will similarly control the subcellular compartmentalization of other GAF domain-containing PDE families, given recent reports showing GAF-B mutations change the subcellular compartmentalization of PDE6C (effect on oligomerization not directly assessed) [68].

A nonsynonymous coding SNP falling within the GAF-B homodimerization domain encodes an alanine at amino acid 499 in C57BL/6J mice but a threonine in BALB/cJ mice. *In vitro* experiments show changing amino acid 499 from an alanine (499A) to a threonine (499T) or a phosphomimic aspartate (499D) promotes homodimerization (Figure 3D, F) and increases trafficking of PDE11A4 into aggregates (Figure 3H-I). Further, 499T/D shifts PDE11A4 from the cytosol to the membrane (Figure 3L, N), perfectly replicating *in vivo* PDE11A4 expression observed in VHIPP of BALB/cJ vs. C57BL/6J mice (Figure 2C). In contrast, disrupting homodimerization using an isolated GAF-B domain (Figure 3E, G) decreases trafficking of PDE11A4 into aggregates (Figure 3J), shifts PDE11A4 from the membrane to the cytosol (Figure 3M, O), and blocks the effect of the 499T and 499D mutations (Figure 3K). Indeed, homodimerization appears to regulate the subcellular compartmentalization of several proteins, including extracellular signal-regulated kinase 2 [69], PleD [70], and Islet-Brain 1 [71]. Differences in protein translation efficiency may also contribute to strain differences in PDE11A4 protein expression as it is a major factor controlling the relative protein expression levels of PDE6 subunits in the retina [72].

PDE11A4 expression and compartmentalization differ between DHIPP and VHIPP

We and others have shown in multiple mouse and rat strains that *Pde11a4* mRNA and protein are enriched in the hippocampus, with expression that is substantially higher in VHIPP vs. DHIPP [4-6, 42, 73, 74]. Here, we noted for the first time a mouse strain (i.e., BALB/cJ) in which *Pde11a4* mRNA expression in DHIPP was equivalent to that in VHIPP (Figure 1A, S1). Even though PDE11A4 mRNA expression did not differ between DHIPP and VHIPP in the BALB/cJ, PDE11A4 protein did show its typical dorsal-ventral gradient at the protein level in this mouse strain (Figure 1D-E, S2C-D). The molecular mechanisms driving these dorsal-ventral gradients in mRNA and protein expression remain to be determined. Preliminary evidence from our laboratory suggests the dorsal-ventral gradient in mRNA expression seen in most mouse and rat strains characterized to date is driven by transcriptional regulation of the promoter, as demonstrated by differential DHIPP vs. VHIPP expression of an mCherry-reporter construct driven by the C57BL/6J PDE11A4 promoter (MP Kelly, personal observations). Indeed, *Sox-5*—a putative PDE11A4 transcription factor [3]—is expressed at significantly higher levels in VHIPP vs. DHIPP [73].

There is also a distinction between DHIPP vs. VHIPP in terms of the subcellular compartments that show PDE11A4 protein expression differences between the mouse strains. In DHIPP, PDE11A4 expression differs between the strains in both cytosolic and membrane compartments, but in VHIPP PDE11A4 expression differs between C57BL/6J and BALB/cJ mice only in the membrane compartment. Again, the mechanism for this remains to be determined, but we hypothesize that phosphorylation of 499T in the BALB/cJ may make PDE11A4 more or less susceptible to other posttranslational modifications whose key modifying enzymes show differential expression along the DHIPP-VHIPP axis. Indeed, preliminary evidence from our lab shows that phosphorylation of one site (e.g., S162) within the PDE11A4 N-terminal domain affects the phosphorylation of other N-terminal sites (e.g., S117 and S124) as well as the functional consequences of those phosphorylation events (W Capell and MP Kelly, personal observations). Interestingly, protein kinase C (PKC) is expressed at much higher levels in DHIPP vs. VHIPP [73] and is predicted to phosphorylate PDE11A4 at the aforementioned N-terminal residues [5]. Exploring this hypothesis will be of interest to future studies.

Pde11a deletion is sufficient to increase lithium responsivity

Pde11a KO mice were more sensitive than WT mice to the effects of lithium in both TST and amphetamine-stimulated hyperactivity. This is consistent with the fact that the C57BL/6J and 129S6/SvEvTac mice with low PDE11A4 expression are more sensitive to the effects of lithium in TST and forced swim test (FST) than BALB/cJ mice with high PDE11A4 expression (Figure 1-2, S1-S3)[45, 50]. Specifically, following 3 weeks of lithium treatment, C57BL/6J mice demonstrated a significant antidepressant-like effect in both TST and FST, 129S6/SvEvTac mice demonstrated a significant antidepressant-like effect only in FST, and BALB/cJ mice demonstrated no effect in either assay [45]. Similarly, 129S6/SvEvTac mice showed a significant antidepressant-like effect of acute lithium treatment in TST and FST, C57BL/6J mice showed a limited antidepressant-like effect in FST, and BALB/cJ mice showed no effect in either assay. C57BL/6J mice have also shown a significant antimanic-like effect of lithium in amphetamine-stimulated locomotor activity;

whereas, 129S6/SvEvTac mice did not (BALB/cJ mice not tested) [62]. The differential lithium sensitivity of C57BL/6J vs. BALB/cJ mice is observed in both males and females whether reared by their own parents or cross-fostered by the opposite strain, suggesting a genetic difference in the offspring is driving this phenotype as opposed to strain differences in maternal care [50]. Our studies here suggest that differential expression and compartmentalization of PDE11A4 may be at least 1 of those mechanisms.

It is important to note that the differential lithium sensitivity of the *Pde11a* KO mice in TST was only detected in group-housed mice (Figure 4B). Specifically, both *Pde11a* WT and KO mice demonstrated antidepressant-like effects of lithium in TST when single housed, but only *Pde11a* KO mice demonstrated this antidepressant-like effect of lithium when group housed. This may suggest that, even when group housed, *Pde11a* KO mice experience subjective or objective social isolation, making them susceptible to the behavioral effects of lithium in TST. Alternatively, social isolation may decrease PDE11A4 expression in the WTs, making them susceptible to the effects of lithium in TST. Indeed, studies currently underway in our laboratory show that social isolation decreases PDE11A4 protein expression and increases IL-6 expression in a subcellular compartment-specific manner (MP Kelly, personal observations). In this context it is interesting to note that lithium increases social interactions in FMR1 KO mice and their WT counterparts [75]. It will be of interest to future studies to further characterize the effects of lithium in the *Pde11a* KO mice, for example in other antidepressant-predictive assays (e.g., FST [45, 50]) or in the context of manipulations intended to model aspects of bipolar disorder (e.g., amphetamine sensitization [41]), particularly give the limited effect size observed herein in TST.

Reduced PDE11A4 expression may reflect a lithium-sensitive pathophysiology

Lower levels of PDE11A4 may predict better lithium responsiveness either because 1) a state of decreased PDE11A4 expression represents a specific disease state that is most responsive to lithium or 2) because reducing PDE11A4 expression somehow boosts lithium's effects. PDE11A KO mice exhibit a number of behavioral, anatomical, and biochemical phenotypes relevant to psychiatric disease [6]. Previously we reported that PDE11A KO mice exhibit significantly reduced cAMP-PDE activity in ventral hippocampus [6]. We have struggled to measure changes in cAMP at the level of the whole ventral hippocampus [6], we believe due to a signal:noise issue caused by the sparse nature of PDE11A4 expression within the hippocampus (i.e., it is only expressed in a subpopulation of neurons in CA1 and subiculum, not CA3 nor DG; [58]). Interestingly, elevated levels of pCREB have been found in lymphoblasts from lithium-responsive bipolar disorder patients and their relatives compared to healthy controls [24]. Here we were not able to measure a significant increase in pCREB in the PDE11A KO mice when examining the VHIPP as a whole; however, we were able to detect a significant decrease in *Arhgap32* mRNA (a.k.a. p250gap, RICS) when examining ventral CA1 specifically (Figure 4A). *Arhgap32* is a gene that is downregulated by increased pCREB signaling via miR132 [59, 60]. Of interest, *Arhgap32* controls dendritic plasticity and has been genetically linked to the ability to identify/describe moods and feeling, schizophrenia, and autism [76-78]. Increased activation of the cAMP cascade may represent a specific pathophysiology that is particularly

responsive to lithium treatment because chronic lithium appears to decrease pCREB in hippocampus and cortex of rats [79].

Here, C57BL/6J and PDE11A KO mice also exhibit significantly higher levels of the proinflammatory cytokine IL-6 relative to BALB/cJ and WT mice, respectively (Figure 5). Increased IL-6 and/or IL-6 receptor expression is not selectively associated with bipolar disorder but has been repeatedly observed in patients with mania, depression, and suicidal ideation [30-34, 36, 37], and lithium decreases IL-6 expression in patient tissue [35]. In addition, PDE11A KO mice and IPSC-derived hippocampal neurons from bipolar patients exhibit altered signaling in the neuroactive-ligand receptor pathway and increased neural activity [6, 16, 80]. Together, these data argue that a state of decreased PDE11A4 expression represents a lithium-responsive pathophysiology. That said, lithium decreases *PDE11A* mRNA expression in IPSC-derived hippocampal neurons from lithium-responsive patients but not non-responsive patients, which is consistent with the idea that lowering PDE11A is key to the therapeutic actions of lithium [16]. One possible explanation for these dichotomous results is the fact that the IPSC-derived hippocampal neurons were described as dentate gyrus (DG) granule cell-like neurons; however, endogenous PDE11A4 in the rodent brain is expressed in CA1 and subiculum, but not DG. Thus, it will be critical for future studies to determine which, if any, isoform of PDE11A is expressed *in vivo* in the human dentate gyrus, what functional implications that would hold for the hippocampal circuit, and exactly why lowering PDE11A expression is sufficient to increase lithium responsiveness.

Supplementary Material

Refer to Web version on PubMed Central for supplementary material.

ACKNOWLEDGEMENTS

The authors would like to thank Jennifer Klett for technical assistance and Drs. John Kelsoe and Susan Leckband for helpful discussion.

FINANCIAL DISCLOSURES: Research supported by a Research Starter Grant in Pharmacology & Toxicology from the PhRMA Foundation, an ASPIRE award from the Office of the Vice President for Research from the University of South Carolina, a Research Development Fund Award from the University of South Carolina School of Medicine, 1R01MH101130 from NIMH, and a NARSAD Young Investigator Award from the Brain & Behavior Research Foundation (all awards to MPK).

REFERENCES [remember to go through and correct formatting]

- [1]. Malhi GS, Tanius M, Das P, Berk M. The science and practice of lithium therapy. *Aust N Z J Psychiatry*. 2012; 46:192–211. [PubMed: 22391277]
- [2]. Yuasa K, Ohgaru T, Asahina M, Omori K. Identification of rat cyclic nucleotide phosphodiesterase 11A (PDE11A): comparison of rat and human PDE11A splicing variants. *Eur J Biochem*. 2001; 268:4440–8. [PubMed: 11502204]
- [3]. Yuasa K, Kanoh Y, Okumura K, Omori K. Genomic organization of the human phosphodiesterase PDE11A gene. Evolutionary relatedness with other PDEs containing GAF domains. *Eur J Biochem*. 2001; 268:168–78. [PubMed: 11121118]
- [4]. Kelly MP, Adamowicz W, Bove S, Hartman AJ, Mariga A, Pathak G, et al. Select 3',5'-cyclic nucleotide phosphodiesterases exhibit altered expression in the aged rodent brain. *Cell Signal*. 2014; 26:383–97. [PubMed: 24184653]

- [5]. Kelly MP. Does phosphodiesterase 11A (PDE11A) hold promise as a future therapeutic target? *Curr Pharm Des.* 2015; 21:389–416. [PubMed: 25159071]
- [6]. Kelly MP, Logue SF, Brennan J, Day JP, Lakkaraju S, Jiang L, et al. Phosphodiesterase 11A in brain is enriched in ventral hippocampus and deletion causes psychiatric disease-related phenotypes. *Proc Natl Acad Sci U S A.* 2010; 107:8457–62. [PubMed: 20404172]
- [7]. Wong ML, Whelan F, Deloukas P, Whittaker P, Delgado M, Cantor RM, et al. Phosphodiesterase genes are associated with susceptibility to major depression and antidepressant treatment response. *Proc Natl Acad Sci U S A.* 2006; 103:15124–9. [PubMed: 17008408]
- [8]. Luo HR, Wu GS, Dong C, Arcos-Burgos M, Ribeiro L, Licinio J, et al. Association of PDE11A global haplotype with major depression and antidepressant drug response. *Neuropsychiatr Dis Treat.* 2009; 5:163–70. [PubMed: 19557111]
- [9]. Cabanero M, Laje G, Detera-Wadleigh S, McMahon FJ. Association study of phosphodiesterase genes in the Sequenced Treatment Alternatives to Relieve Depression sample. *Pharmacogenet Genomics.* 2009; 19:235–8. [PubMed: 19214142]
- [10]. Couzin J. Science and commerce. Gene tests for psychiatric risk polarize researchers. *Science.* 2008; 319:274–7. [PubMed: 18202268]
- [11]. Kelsoe, J. Office UPT. THE REGENTS OF THE UNIVERSITY OF CALIFORNIA (Oakland, CA): USA: 2010. METHOD TO PREDICT RESPONSE TO TREATMENT FOR PSYCHIATRIC ILLNESSES; p. 1
- [12]. Coon H, Darlington T, Pimentel R, Smith KR, Huff CD, Hu H, et al. Genetic risk factors in two Utah pedigrees at high risk for suicide. *Transl Psychiatry.* 2013; 3:e325. [PubMed: 24252905]
- [13]. Laje G, Perlis RH, Rush AJ, McMahon FJ. Pharmacogenetics studies in STAR*D: strengths, limitations, and results. *Psychiatr Serv.* 2009; 60:1446–57. [PubMed: 19880459]
- [14]. Perlis RH, Fijal B, Dharia S, Heinloth AN, Houston JP. Failure to replicate genetic associations with antidepressant treatment response in duloxetine-treated patients. *Biol Psychiatry.* 2010; 67:1110–3. [PubMed: 20110084]
- [15]. Malhi GS, Tanious M, Das P, Coulston CM, Berk M. Potential mechanisms of action of lithium in bipolar disorder. Current understanding. *CNS Drugs.* 2013; 27:135–53. [PubMed: 23371914]
- [16]. Mertens J, Wang QW, Kim Y, Yu DX, Pham S, Yang B, et al. Differential responses to lithium in hyperexcitable neurons from patients with bipolar disorder. *Nature.* 2015; 527:95–9. [PubMed: 26524527]
- [17]. Gould TD, Quiroz JA, Singh J, Zarate CA, Manji HK. Emerging experimental therapeutics for bipolar disorder: insights from the molecular and cellular actions of current mood stabilizers. *Mol Psychiatry.* 2004; 9:734–55. [PubMed: 15136794]
- [18]. Rahman S, Li PP, Young LT, Kofman O, Kish SJ, Warsh JJ. Reduced [3H]cyclic AMP binding in postmortem brain from subjects with bipolar affective disorder. *J Neurochem.* 1997; 68:297–304. [PubMed: 8978738]
- [19]. Avissar S, Nechamkin Y, Barki-Harrington L, Roitman G, Schreiber G. Differential G protein measures in mononuclear leukocytes of patients with bipolar mood disorder are state dependent. *J Affect Disord.* 1997; 43:85–93. [PubMed: 9165378]
- [20]. Avissar S, Schreiber G. The involvement of G proteins and regulators of receptor-G protein coupling in the pathophysiology, diagnosis and treatment of mood disorders. [Review] [109 refs]. *Clinica Chimica Acta.* 2006; 366:37–47.
- [21]. Schreiber G, Avissar S. Lithium sensitive G protein hyperfunction: a dynamic model for the pathogenesis of bipolar affective disorder. *Med Hypotheses.* 1991; 35:237–43. [PubMed: 1943867]
- [22]. Schreiber G, Avissar S, Danon A, Belmaker RH. Hyperfunctional G proteins in mononuclear leukocytes of patients with mania. *Biological Psychiatry.* 1991; 29:273–280. [PubMed: 1901735]
- [23]. Fields A, Li PP, Kish SJ, Warsh JJ. Increased cyclic AMP-dependent protein kinase activity in postmortem brain from patients with bipolar affective disorder. *Journal of Neurochemistry.* 1999; 73:1704–1710. [PubMed: 10501218]
- [24]. Alda M, Shao L, Wang JF, Lopez de Lara C, Jaitovich-Groisman I, Lebel V, et al. Alterations in phosphorylated cAMP response element-binding protein (pCREB) signaling: an endophenotype of lithium-responsive bipolar disorder? *Bipolar Disord.* 2013; 15:824–31. [PubMed: 24238631]

- [25]. Chang A, Li PP, Warsh JJ. Altered cAMP-dependent protein kinase subunit immunolabeling in post-mortem brain from patients with bipolar affective disorder.[erratum appears in J Neurochem. 2003 Apr;85(1):286.]. *Journal of Neurochemistry*. 2003; 84:781–791. [PubMed: 12562522]
- [26]. Dowlatshahi D, MacQueen GM, Wang JF, Reiaich JS, Young LT. G Protein-coupled cyclic AMP signaling in postmortem brain of subjects with mood disorders: effects of diagnosis, suicide, and treatment at the time of death. *J Neurochem*. 1999; 73:1121–6. [PubMed: 10461903]
- [27]. Mori S, Tardito D, Dorigo A, Zanardi R, Smeraldi E, Racagni G, et al. Effects of lithium on cAMP-dependent protein kinase in rat brain. *Neuropsychopharmacology*. 1998; 19:233–40. [PubMed: 9653711]
- [28]. Jensen JB, Mork A. Altered protein phosphorylation in the rat brain following chronic lithium and carbamazepine treatments. *Eur Neuropsychopharmacol*. 1997; 7:173–9. [PubMed: 9213075]
- [29]. Casebolt TL, Jope RS. Effects of chronic lithium treatment on protein kinase C and cyclic AMP-dependent protein phosphorylation. *Biol Psychiatry*. 1991; 29:233–43. [PubMed: 2015330]
- [30]. Dowlati Y, Herrmann N, Swardfager W, Liu H, Sham L, Reim EK, et al. A meta-analysis of cytokines in major depression. *Biol Psychiatry*. 2010; 67:446–57. [PubMed: 20015486]
- [31]. Maes M, Bosmans E, De Jongh R, Kenis G, Vandoolaeghe E, Neels H. Increased serum IL-6 and IL-1 receptor antagonist concentrations in major depression and treatment resistant depression. *Cytokine*. 1997; 9:853–8. [PubMed: 9367546]
- [32]. Maes M, Bosmans E, Calabrese J, Smith R, Meltzer HY. Interleukin-2 and interleukin-6 in schizophrenia and mania: effects of neuroleptics and mood stabilizers. *J Psychiatr Res*. 1995; 29:141–52. [PubMed: 7666381]
- [33]. Brietzke E, Stertz L, Fernandes BS, Kauer-Sant'anna M, Mascarenhas M, Escosteguy Vargas A, et al. Comparison of cytokine levels in depressed, manic and euthymic patients with bipolar disorder. *J Affect Disord*. 2009; 116:214–7. [PubMed: 19251324]
- [34]. Simon NM, McNamara K, Chow CW, Maser RS, Papakostas GI, Pollack MH, et al. A detailed examination of cytokine abnormalities in Major Depressive Disorder. *Eur Neuropsychopharmacol*. 2008; 18:230–3. [PubMed: 17681762]
- [35]. Watanabe S, Iga J, Nishi A, Numata S, Kinoshita M, Kikuchi K, et al. Microarray analysis of global gene expression in leukocytes following lithium treatment. *Hum Psychopharmacol*. 2014; 29:190–8. [PubMed: 24590544]
- [36]. Niculescu AB, Levey DF, Phalen PL, Le-Niculescu H, Dainton HD, Jain N, et al. Understanding and predicting suicidality using a combined genomic and clinical risk assessment approach. *Mol Psychiatry*. 2015
- [37]. Khandaker GM, Pearson RM, Zammit S, Lewis G, Jones PB. Association of serum interleukin 6 and C-reactive protein in childhood with depression and psychosis in young adult life: a population-based longitudinal study. *JAMA Psychiatry*. 2014; 71:1121–8. [PubMed: 25133871]
- [38]. Stephenson DT, Coskran TM, Kelly MP, Kleiman RJ, Morton D, O'Neill SM, et al. The distribution of phosphodiesterase 2A in the rat brain. *Neuroscience*. 2012; 226:145–55. [PubMed: 23000621]
- [39]. Charych EI, Jiang LX, Lo F, Sullivan K, Brandon NJ. Interplay of palmitoylation and phosphorylation in the trafficking and localization of phosphodiesterase 10A: implications for the treatment of schizophrenia. *J Neurosci*. 2010; 30:9027–37. [PubMed: 20610737]
- [40]. Sukoff Rizzo SJ, Neal SJ, Hughes ZA, Beyna M, Rosenzweig-Lipson S, Moss SJ, et al. Evidence for sustained elevation of IL-6 in the CNS as a key contributor of depressive-like phenotypes. *Transl Psychiatry*. 2012; 2:e199.
- [41]. Pathak G, Ibrahim BA, McCarthy SA, Baker K, Kelly MP. Amphetamine sensitization in mice is sufficient to produce both manic- and depressive-related behaviors as well as changes in the functional connectivity of corticolimbic structures. *Neuropharmacology*. 2015; 95:434–447. [PubMed: 25959066]
- [42]. Kelly, MP. Putting together the pieces of phosphodiesterase distribution patterns in the brain: A jigsaw puzzle of cyclic nucleotide regulation. In: Brandon, NJ., West, AR., editors. *Cyclic Nucleotide Phosphodiesterases in the Central Nervous System: From Biology to Disease*. John Wiley & Sons, Inc; New Jersey: 2014.

- [43]. Jackson RJ, Howell MT, Kaminski A. The novel mechanism of initiation of picornavirus RNA translation. *Trends Biochem Sci.* 1990; 15:477–83. [PubMed: 2077688]
- [44]. Shaner NC, Campbell RE, Steinbach PA, Giepmans BN, Palmer AE, Tsien RY. Improved monomeric red, orange and yellow fluorescent proteins derived from *Discosoma* sp. red fluorescent protein. *Nat Biotechnol.* 2004; 22:1567–72. [PubMed: 15558047]
- [45]. Can A, Blackwell RA, Piantadosi SC, Dao DT, O'Donnell KC, Gould TD. Antidepressant-like responses to lithium in genetically diverse mouse strains. *Genes Brain Behav.* 2011; 10:434–43. [PubMed: 21306560]
- [46]. Kelly MP, Logue SF, Dwyer JM, Beyer CE, Majchrowski H, Cai Z, et al. The supra-additive hyperactivity caused by an amphetamine-chlordiazepoxide mixture exhibits an inverted-U dose response: negative implications for the use of a model in screening for mood stabilizers. *Pharmacol Biochem Behav.* 2009; 92:649–54. [PubMed: 19303035]
- [47]. Hughes ZA, Liu F, Platt BJ, Dwyer JM, Pulicicchio CM, Zhang G, et al. WAY-200070, a selective agonist of estrogen receptor beta as a potential novel anxiolytic/antidepressant agent. 2008; 54:1136–1142.
- [48]. Malberg JE, Platt B, Rizzo SJ, Ring RH, Lucki I, Schechter LE, et al. Increasing the levels of insulin-like growth factor-I by an IGF binding protein inhibitor produces anxiolytic and antidepressant-like effects. *Neuropsychopharmacology.* 2007; 32:2360–8. [PubMed: 17342171]
- [49]. Kelly MP, Cheung YF, Favilla C, Siegel SJ, Kaness SJ, Houslay MD, et al. Constitutive activation of the G-protein subunit α within forebrain neurons causes PKA-dependent alterations in fear conditioning and cortical Arc mRNA expression. *Learn Mem.* 2008; 15:75–83. [PubMed: 18230676]
- [50]. Can A, Piantadosi SC, Gould TD. Differential antidepressant-like response to lithium treatment between mouse strains: effects of sex, maternal care, and mixed genetic background. *Psychopharmacology (Berl).* 2013; 228:411–8. [PubMed: 23503701]
- [51]. Karolchik D, Barber GP, Casper J, Clawson H, Cline MS, Diekhans M, et al. The UCSC Genome Browser database: 2014 update. *Nucleic Acids Res.* 2014; 42:D764–70. [PubMed: 24270787]
- [52]. Bogue MA, Peters LL, Paigen B, Korstanje R, Yuan R, Ackert-Bicknell C, et al. Accessing Data Resources in the Mouse Phenome Database for Genetic Analysis of Murine Life Span and Health Span. *J Gerontol A Biol Sci Med Sci.* 2014
- [53]. Sherry ST, Ward MH, Kholodov M, Baker J, Phan L, Smigielski EM, et al. dbSNP: the NCBI database of genetic variation. *Nucleic Acids Res.* 2001; 29:308–11. [PubMed: 11125122]
- [54]. Chaney JL, Clark PL. Roles for Synonymous Codon Usage in Protein Biogenesis. *Annu Rev Biophys.* 2015; 44:143–66. [PubMed: 25747594]
- [55]. Weeks JL 2nd, Zoraghi R, Francis SH, Corbin JD. N-Terminal domain of phosphodiesterase-11A4 (PDE11A4) decreases affinity of the catalytic site for substrates and tadalafil, and is involved in oligomerization. *Biochemistry.* 2007; 46:10353–64. [PubMed: 17696499]
- [56]. Edwards HV, Christian F, Baillie GS. cAMP: novel concepts in compartmentalised signalling. *Semin Cell Dev Biol.* 2012; 23:181–90. [PubMed: 21930230]
- [57]. McCahill AC, Huston E, Li X, Houslay MD. PDE4 associates with different scaffolding proteins: modulating interactions as treatment for certain diseases. *Handb Exp Pharmacol.* 2008:125–66. [PubMed: 18491051]
- [58]. Hegde S, Capell WR, Ibrahim BA, Klett J, Patel NS, Sougiannis AT, et al. Phosphodiesterase 11A4 (PDE11A4) in hippocampus is required for the consolidation of social but not non-social memories. *Neuropsychopharmacology.* in press.
- [59]. Wayman GA, Davare M, Ando H, Fortin D, Varlamova O, Cheng HY, et al. An activity-regulated microRNA controls dendritic plasticity by down-regulating p250GAP. *Proc Natl Acad Sci U S A.* 2008; 105:9093–8. [PubMed: 18577589]
- [60]. Dhar M, Zhu M, Impey S, Lambert TJ, Bland T, Karatsoreos IN, et al. Leptin induces hippocampal synaptogenesis via CREB-regulated microRNA-132 suppression of p250GAP. *Mol Endocrinol.* 2014; 28:1073–87. [PubMed: 24877561]
- [61]. Steru L, Chermat R, Thierry B, Simon P. The tail suspension test: a new method for screening antidepressants in mice. *Psychopharmacology (Berl).* 1985; 85:367–70. [PubMed: 3923523]

- [62]. Gould TD, O'Donnell KC, Picchini AM, Manji HK. Strain differences in lithium attenuation of d-amphetamine-induced hyperlocomotion: a mouse model for the genetics of clinical response to lithium. *Neuropsychopharmacology*. 2007; 32:1321–1333. [PubMed: 17151598]
- [63]. Gould TJ, Keith RA, Bhat RV. Differential sensitivity to lithium's reversal of amphetamine-induced open-field activity in two inbred strains of mice. *Behavioural Brain Research*. 2001; 118:95–105. [PubMed: 11163638]
- [64]. Fatemi SH, Folsom TD, Reutiman TJ, Vazquez G. Phosphodiesterase signaling system is disrupted in the cerebella of subjects with schizophrenia, bipolar disorder, and major depression. *Schizophr Res*. 2010; 119:266–7. [PubMed: 20299190]
- [65]. Fatemi SH, Reutiman TJ, Folsom TD, Lee S. Phosphodiesterase-4A expression is reduced in cerebella of patients with bipolar disorder. *Psychiatr Genet*. 2008; 18:282–8. [PubMed: 19018233]
- [66]. Sun X, Young LT, Wang JF, Grof P, Turecki G, Rouleau GA, et al. Identification of lithium-regulated genes in cultured lymphoblasts of lithium responsive subjects with bipolar disorder. *Neuropsychopharmacology*. 2004; 29:799–804. [PubMed: 14735134]
- [67]. Francis SH, Blount MA, Corbin JD. Mammalian cyclic nucleotide phosphodiesterases: molecular mechanisms and physiological functions. *Physiol Rev*. 2011; 91:651–90. [PubMed: 21527734]
- [68]. Cheguru P, Majumder A, Artemyev NO. Distinct patterns of compartmentalization and proteolytic stability of PDE6C mutants linked to achromatopsia. *Mol Cell Neurosci*. 2015; 64:1–8. [PubMed: 25461672]
- [69]. Khokhlatchev AV, Canagarajah B, Wilsbacher J, Robinson M, Atkinson M, Goldsmith E, et al. Phosphorylation of the MAP kinase ERK2 promotes its homodimerization and nuclear translocation. *Cell*. 1998; 93:605–15. [PubMed: 9604935]
- [70]. Paul R, Abel S, Wassmann P, Beck A, Heerklotz H, Jenal U. Activation of the diguanylate cyclase PleD by phosphorylation-mediated dimerization. *J Biol Chem*. 2007; 282:29170–7. [PubMed: 17640875]
- [71]. Borsello T, Centeno C, Riederer IM, Haefliger JA, Riederer BM. Phosphorylation-dependent dimerization and subcellular localization of islet-brain 1/c-Jun N-terminal kinase-interacting protein 1. *J Neurosci Res*. 2007; 85:3632–41. [PubMed: 17663463]
- [72]. Piri N, Yamashita CK, Shih J, Akhmedov NB, Farber DB. Differential expression of rod photoreceptor cGMP-phosphodiesterase alpha and beta subunits: mRNA and protein levels. *J Biol Chem*. 2003; 278:36999–7005. [PubMed: 12871955]
- [73]. Cembrowski MS, Bachman JL, Wang L, Sugino K, Shields BC, Spruston N. Spatial Gene-Expression Gradients Underlie Prominent Heterogeneity of CA1 Pyramidal Neurons. *Neuron*. 2016
- [74]. Jager R, Russwurm C, Schwede F, Genieser HG, Koesling D, Russwurm M. Activation of PDE10 and PDE11 phosphodiesterases. *J Biol Chem*. 2012; 287:1210–9. [PubMed: 22105073]
- [75]. Liu ZH, Chuang DM, Smith CB. Lithium ameliorates phenotypic deficits in a mouse model of fragile X syndrome. *Int J Neuropsychopharmacol*. 2011; 14:618–30. [PubMed: 20497624]
- [76]. Ohi K, Hashimoto R, Nakazawa T, Okada T, Yasuda Y, Yamamori H, et al. The p250GAP gene is associated with risk for schizophrenia and schizotypal personality traits. *PLoS One*. 2012; 7:e35696. [PubMed: 22530067]
- [77]. Akshoomoff N, Mattson SN, Grossfeld PD. Evidence for autism spectrum disorder in Jacobsen syndrome: identification of a candidate gene in distal 11q. *Genet Med*. 2015; 17:143–8. [PubMed: 25058499]
- [78]. Mezzavilla M, Ulivi S, Bianca ML, Carlino D, Gasparini P, Robino A. Analysis of functional variants reveals new candidate genes associated with alexithymia. *Psychiatry Res*. 2015; 227:363–5. [PubMed: 25882097]
- [79]. Chen B, Wang JF, Hill BC, Young LT. Lithium and valproate differentially regulate brain regional expression of phosphorylated CREB and c-Fos. *Brain Res Mol Brain Res*. 1999; 70:45–53. [PubMed: 10381542]
- [80]. Hegde S, Oliver D, Poupore N, Shtutman M, Kelly MP. Pde11a is required for intact social behaviors and is a key mechanism by which social experience sculpts the brain. 2016 submitted.

- [81]. Blount MA, Beasley A, Zoraghi R, Sekhar KR, Bessay EP, Francis SH, et al. Binding of tritiated sildenafil, tadalafil, or vardenafil to the phosphodiesterase-5 catalytic site displays potency, specificity, heterogeneity, and cGMP stimulation. *Mol Pharmacol.* 2004; 66:144–52. [PubMed: 15213306]

Author Manuscript

Author Manuscript

Author Manuscript

Author Manuscript

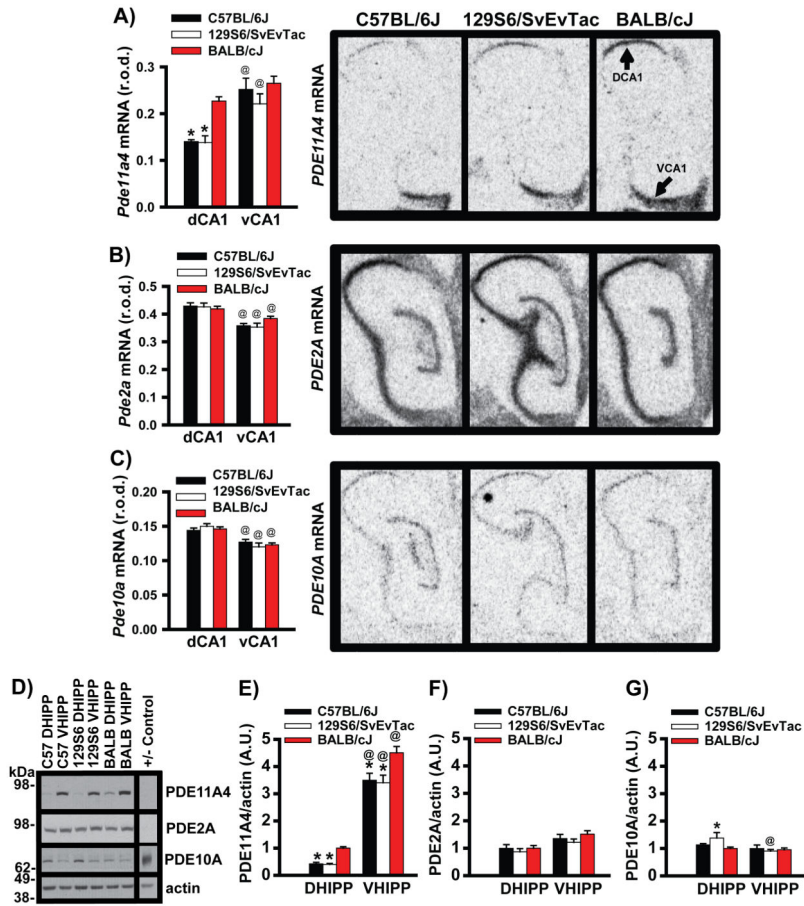


Figure 1. C57BL/6J mice express significantly lower levels of PDE11A4 mRNA than do BALB/cJ mice

To determine if lithium responsiveness may correlate with PDE11A expression across mouse strains, we measured PDE11A4 expression in hippocampi taken from mice that respond well (C57BL/6J), moderately well (129S6/SvEvTac), or poorly to chronic lithium (BALB/cJ). A) PDE11A4 mRNA expression in the C57BL/6J (n=7) and 129S6/SvEvTac mice (n=7) is significantly lower than that in the BALB/cJ mice (n=6); however, this difference in mRNA expression is restricted to dorsal CA1 (DCA1). Data is shown for the oligonucleotide probe that selectively recognizes the PDE11A4 isoform, but is representative of results obtained with 3 different oligonucleotide probes (see Figure S1 for data collected in a second cohort). Surprisingly, BALB/cJ mice fail to show the typical enrichment of PDE11A4 mRNA expression in ventral CA1 (VCA1) vs. DCA1, as has been previously reported in mice and rats and can be seen here in the C57BL/6J mice and 129S6/SvEvTac mice. B) The expression of PDE2A and C) PDE10A mRNA are not significantly different between strains, suggesting specificity of the PDE11A4 effect. D) Western blots measuring PDE11A4 (–control = PDE11A KO VHIPP), PDE2A (– control = cerebellum), PDE10A (+ control = striatum), and actin. E) C57BL/6J and 129S6/SvEvTac mice express significantly less PDE11A4 protein relative to BALB/cJ mice in both DHIPP and VHIPP (n=12/strain). Further, all 3 strains demonstrate far more expression of PDE11A4 protein in VHIPP vs. DHIPP, despite the lack of difference at the mRNA level in the BALB/cJ mice. These effects

were replicated in a second cohort of mice (Figure S2). F) Neither PDE2A nor G) PDE10A protein expression differ between the strains, again suggesting specificity of the PDE11A4 effect. *Post hoc*, * vs BALB/cJ, $P < 0.001$; @ vs DCA1 or DHIPP, $P < 0.017-0.001$. R.O.D.—relative optical density. A.U.—arbitrary units. Data pass normality and equal variance and are graphed as means \pm SEM. Brightness and contrast adjusted for graphical clarity of autoradiograph and Western blot images.

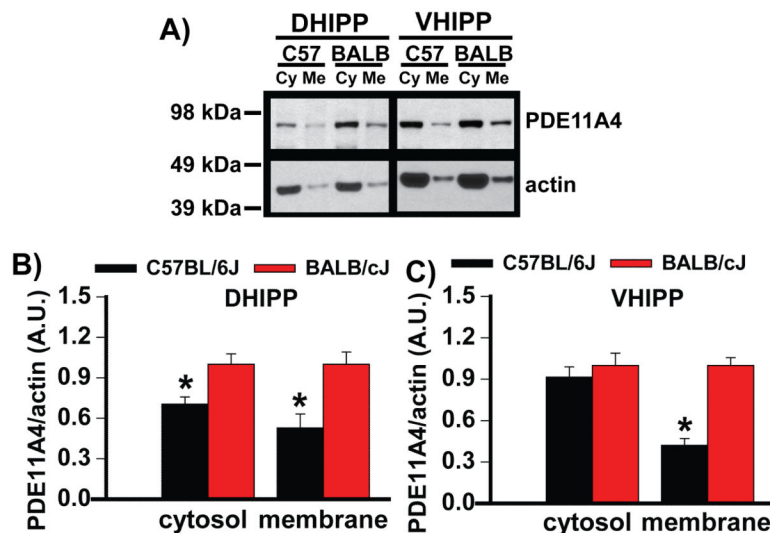


Figure 2. C57BL/6J mice compartmentalize PDE11A4 protein in VHIPP differently than do BALB/cJ mice

To determine if PDE11A4 protein expression differences between C57BL/6J and BALB/cJ mice might be specific to select subcellular compartments, DHIPP and VHIPP samples were biochemically fractionated and then A) probed by Western Blot. B) C57BL/6J mice showed lower PDE11A4 protein expression relative to BALB/cJ mice in both the cytosolic and membrane compartments of the DHIPP, C) but only in the membrane compartment of the VHIPP. This effect was replicated in a second cohort of mice (Figure S3). DHIPP, n=6/strain for membrane and 8/strain for cytosol; VHIPP, n=8/strain per compartment. *Post hoc*, *vs BALB/cJ, P<0.01-0.001, #vs cytosol, P<0.001. Data sets passed normality and equal variance and are graphed as means \pm SEM. Brightness and contrast adjusted for graphical clarity of blot images.

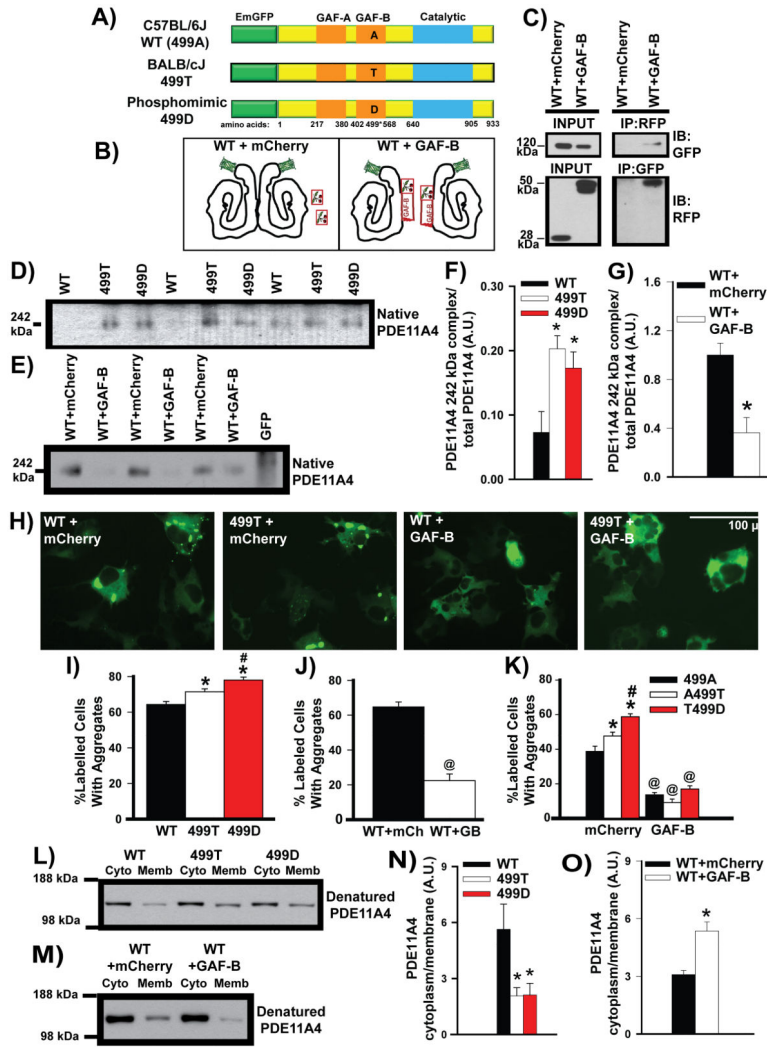


Figure 3. A nonsynonymous coding SNP in the PDE11A4 GAF-B domain promotes PDE11A4 homodimerization and alters PDE11A4 compartmentalization

The PDE11A rs27963339 polymorphism affecting amino acid 499 results in an alanine (499A) in C57BL/6J mice (referred to as wild-type (WT) as this is the sequence published in NCBI) and a threonine (499T) in BALB/cJ mice. A) COS-1 cells were transiently transfected with plasmids encoding an EmGFP-PDE11A4 fusion protein containing a WT 499A, 499T, or 499D (i.e., a phosphomimic aspartate). B) Alternatively, WT PDE11A4 was co-transfected with either mCherry alone or an isolated GAF-B domain fused to mCherry. Hypothetical structure of PDE11A4 based on [81]. C) Co-immunoprecipitation shows that the isolated GAF-B domain binds full-length PDE11A4, enabling the isolated GAF-B domain to act as a dominant negative that prevents homodimerization. D,F) Native PAGE shows that the 499T and 499D mutations increase expression of the presumed homodimer at 252 kDa (n=4/group); whereas, E,G) expression of the isolated GAF-B domain decreases expression of the presumed homodimer (n=6/group). Note: The difference in intensity between the WT vs WT-mCherry groups is not related to the co-expression of mCherry but rather reflects the fact that the experiments were conducted separately and different film exposures were necessary for each experiment in order to keep each group of samples within

the linear range of the film (e.g., if WT and WT-mCherry exposures were kept constant between experiments, then the 499 groups would be overexposed). H, I) Consistent with these opposing effects on homodimerization, 499T and 499D promote aggregation of PDE11A4 in COS-1 cells (n=8/group); whereas, J) the isolated GAF-B domain decreases aggregation (n=6/group). K) Importantly, the ability of 499T and 499D to promote PDE11A4 aggregation is blocked when homodimerization is prevented by the isolated GAF-B domain (n=8/group), which suggests the ability of 499T and 499D to increase homodimerization is directly related to their ability to promote the trafficking of PDE11A4 into aggregates. L, N) Biochemical fractionations show that 499T and 499D shift PDE11A4 from the cytosol to the membrane relative to WT PDE11A4 (n=5/group), mimicking PDE11A4 compartmentalization in the VHIPP of BALB/cJ vs. C57BL/6J mice. M,O). In contrast, disrupting homodimerization with the isolated GAF-B domain shifts PDE11A4 from the membrane to the cytosol (mCherry, n=13; GAF-B, n=9). The fact that 499T and 499D behave similarly suggests the 499T construct is naturally phosphorylated in COS-1 cells. *Post hoc*, *vs. WT, $P < 0.05-0.001$; #vs. 499T, $P = 0.037-0.011$; @vs. mCherry, $P < 0.001$. A.U.—arbitrary units. Note that all n's reflect biological replicates. Data passed normality and equal variance and are graphed as means \pm SEM. Brightness and contrast adjusted for graphical clarity of images.

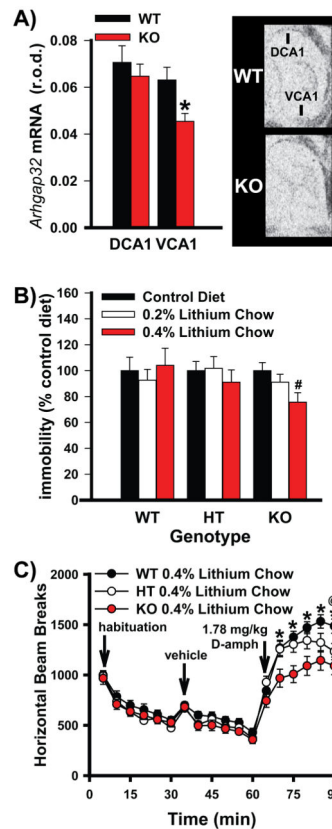


Figure 4. Genetic deletion of PDE11A in mice triggers alterations in the cAMP signaling pathway and increases sensitivity to the antidepressant and anti-manic effects of lithium

A) Autoradiographic *in situ* hybridization shows that PDE11A KO mice exhibit a significant reduction in Arhgap32 mRNA specifically within ventral CA1 (VCA1) relative to wild-type (WT) littermates (n=9/genotype), indicative of localized increases in pCREB signaling [59, 60]. B) PDE11A KO mice chronically fed 0.4% lithium chow (n=15), but not 0.2% lithium chow (n=21) demonstrated a significant antidepressant-like reduction in tail suspension test (TST) immobility relative to PDE11A KO mice fed a control diet (n=19). PDE11A WT and HT mice showed no significant change in immobility when fed either 0.4% (WT, n=16; HT, n=16) or 0.2% lithium chow (WT, n=20; HT, n=14) relative to the control diet (WT, n=18; HT, n=16). C) At specific time points, PDE11A KO and PDE11A HT mice chronically fed the 0.4% lithium chow demonstrated a significant antimanic-like attenuation of the amphetamine-stimulated rise in horizontal beam breaks relative to WT littermates (WT and HT, n=26; KO, n=25). *Post hoc*, #vs. control chow, P=0.011; *vs. KO, P=0.015-0.002; @vs. HT, P=0.02. Data passed normality and equal variance and are graphed as means \pm SEM. Brightness and contrast adjusted for graphical clarity of autoradiographic images.

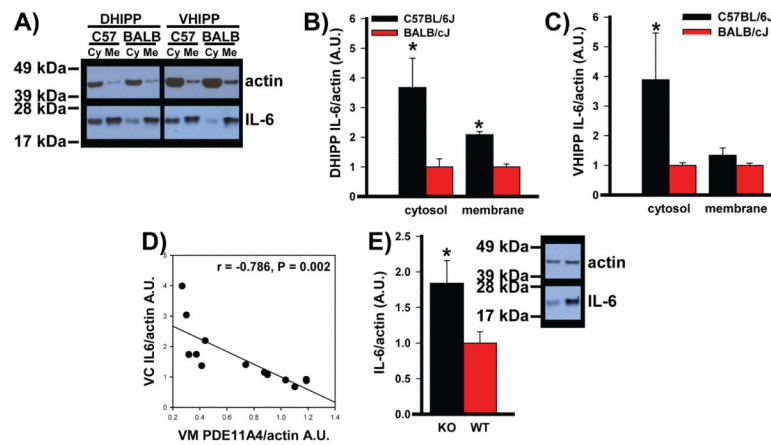


Figure 5. Decreasing PDE11A expression increases IL-6 expression

To determine if decreased PDE11A4 may drive expression of pathophysiological markers, we examined expression of the proinflammatory cytokine IL-6. A) Western blots show that B) C57BL/6J mice express more IL-6 relative to BALB/cJ mice in both the cytosolic and membrane fractions of DHIPP (n=6/strain for membrane and 8/strain for cytosol). C) In VHIPP, however, C57BL/6J mice only express more IL-6 relative to BALB/cJ mice in the cytosolic fraction (n=8/strain/compartments). D) Interestingly, PDE11A4 expression in the VHIPP membrane fraction correlates negatively with IL-6 expression in the VHIPP cytosol, such that C57BL/6J and BALB/cJ mice with lower PDE11A4 expression exhibit higher levels of IL-6 expression. E) Decreasing PDE11A expression appears sufficient to upregulate IL-6 because PDE11A KO mice demonstrate significantly more IL-6 expression relative to paired sex-matched WT littermates in DHIPP (WT, n=17; KO, n=19). Data in panel B passed normality and equal variance. Data in panel C and E failed normality; therefore, nonparametric tests were used for those datasets. Data are graphed as means \pm SEM. Brightness and contrast adjusted for graphical clarity of blot images. *Post hoc*, *vs. BALB/cJ or WT, P 0.005-0.001.